Published in final edited form as:
Neuroimage. 2013 October 1; 79: 223–233. doi:10.1016/j.neuroimage.2013.04.044.

Dominant frequencies of resting human brain activity as measured by the electrocorticogram

David M. Groppe[a], **Stephan Bickel**[b], **Corey J. Keller**[a,c], **Sanjay K. Jain**[d], **Sean T. Hwang**[d], **Cynthia Harden**[d], and **Ashesh D. Mehta**[a,d,*]

[a]Department of Neurosurgery, Hofstra North Shore LIJ School of Medicine and Feinstein Institute for Medical Research, 300 Community Dr., Manhasset, NY 11030, USA

[b]Department of Neurology, Albert Einstein College of Medicine, 1300 Morris Park Ave., Bronx, NY 10461, USA

[c]Department of Neuroscience, Albert Einstein College of Medicine, 1300 Morris Park Ave., Bronx, NY 10461, USA

[d]Department of Neurology and Comprehensive Epilepsy Care Center, Cushing Neuroscience Institute, Hofstra North Shore LIJ School of Medicine, 611 Northern Blvd., Suite 150, Great Neck, NY 11021, USA

Abstract

The brain's spontaneous, intrinsic activity is increasingly being shown to reveal brain function, delineate large scale brain networks, and diagnose brain disorders. One of the most studied and clinically utilized types of intrinsic brain activity are oscillations in the electrocorticogram (ECoG), a relatively localized measure of cortical synaptic activity. Here we objectively characterize the types of ECoG oscillations commonly observed over particular cortical areas when an individual is awake and immobile with eyes closed, using a surface-based cortical atlas and cluster analysis. Both methods show that [1] there is generally substantial variability in the dominant frequencies of cortical regions and substantial overlap in dominant frequencies across the areas sampled (primarily lateral central, temporal, and frontal areas), [2] theta (4–8 Hz) is the most dominant type of oscillation in the areas sampled with a mode around 7 Hz, [3] alpha (8–13 Hz) is largely limited to parietal and occipital regions, and [4] beta (13–30 Hz) is prominent peri-Rolandically, over the middle frontal gyrus, and the pars opercularis. In addition, the cluster analysis revealed seven types of ECoG spectral power densities (SPDs). Six of these have peaks at 3, 5, 7 (narrow), 7 (broad), 10, and 17 Hz, while the remaining cluster is broadly distributed with less pronounced peaks at 8, 19, and 42 Hz. These categories largely corroborate conventional sub-gamma frequency band distinctions (delta, theta, alpha, and beta) and suggest multiple sub-types of theta. Finally, we note that gamma/high gamma activity (30+ Hz) was at times prominently

*Corresponding author at: Dept. of Neurosurgery, North Shore University Hospital, 300 Community Drive, Manhasset, NY 11021, USA. amehta@nshs.edu (A.D. Mehta).

Supplementary data to this article can be found online at http://dx.doi.org/10.1016/j.neuroimage.2013.04.044.

Conflicts of interest
The authors declare no conflicts of interest.

observed, but was too infrequent and variable across individuals to be reliably characterized. These results should help identify abnormal patterns of ECoG oscillations, inform the interpretation of EEG/MEG intrinsic activity, and provide insight into the functions of these different oscillations and the networks that produce them. Specifically, our results support theories of the importance of theta oscillations in general cortical function, suggest that alpha activity is primarily related to sensory processing/attention, and demonstrate that beta networks extend far beyond primary sensorimotor regions.

Keywords

Electrocorticogram; Oscillations; Resting state; Theta; Alpha; Beta

Introduction

Oscillations characteristic of the brain's intrinsic activity

In recent years, the neurosciences have become increasingly interested in understanding the intrinsic activity of the brain (Kelly et al., 2012). This work is well motivated as intrinsic activity, typically measured when an individual is awake and immobile (i.e., in a "resting state"), has proven effective at identifying various functional brain networks (Kokkonen et al., 2009; Power et al., 2011), is likely to serve important functional roles (Raichle, 2006), and may be a biomarker of various neurological and psychiatric disorders (Fox and Greicius, 2010). The longest studied and most clinically utilized types of intrinsic brain activity are oscillations in the electroencephalogram (EEG), magnetoencephalogram (MEG), and intracranial electroencephalogram/electrocorticogram (iEEG/ECoG), which primarily reflect cortical synaptic potentials (Kutas and Dale, 1997). Decades of research on this activity, originally called the "eigenströme" (Penfield and Jasper, 1954), have led to conventional classes of oscillations based on the fact that some of these rhythms are robustly characteristic of particular brain regions, functions and states. The most conventional frequency bands are: delta [1–4 Hz], theta [4–8 Hz], alpha/mu [8–13 Hz], beta [13–30 Hz], gamma [30–80 Hz], and high gamma [80–150 Hz] (Canolty et al., 2006; Crone et al., 2011; MacKay, 1997)[1].

Perhaps the best studied of these rhythms are the occipital alpha and central mu rhythms, since they are clearly observed at the scalp. Occipital alpha is predominantly generated by the occipital cortex and is found to a lesser extent in the parietal and temporal lobes (Feige, 2005; Perez-Borja et al., 1962; Sperling, 1993). It is likely produced by a loop between these cortical areas and the thalamus (Feige, 2005; Rowe et al., 2004), though it may reflect cortico-cortical interactions as well (Nunez et al., 2001). Alpha is increased by inattention and lack of visual input (Nunez et al., 2001) and the perceptibility of visual stimuli depends on alpha phase (Thut et al., 2012). Some interpret alpha as an idling rhythm that self-organizes when cortical areas are disengaged. However, growing evidence that experimental manipulations of alpha affect perception (Jensen and Mazaheri, 2010; Klimesch et al., 2007; Thut et al., 2012) and that alpha phase may modulate local cortical activity (Voytek, 2010)

[1]Note that the boundaries between the different frequency bands can vary slightly across studies.

suggests that it serves an active role in attention and sensory processing and mediates communication between different cortical areas. Mu is in many ways the sensorimotor analog of occipital alpha. It is predominantly generated by the pre- and postcentral gyri (MacKay, 1997; Sperling, 1993) and at least partially reflects the interactions between these areas and the thalamus (MacKay, 1997). Mu amplitude is decreased by movement (MacKay, 1997) and thus, like alpha, it is greatest when the cortical areas generating it are disengaged. Curiously, unlike alpha, it is not yet clear if mu phase modulates overall levels of local cortical activity (Miller et al., 2012).

Beta oscillations, like mu, are prominent in the pre- and postcentral gyri and are reduced at the onset of movement (Jenkinson and Brown, 2011; MacKay, 1997; Ritter et al., 2009). This has led some to speculate that beta acts to suppress the function of motor cortex by synchronizing its activity (Miller et al., 2012). Curiously, following movement onset, beta amplitude rebounds if the movement is sustained, and is enhanced when movements are suppressed (Jenkinson and Brown, 2011). Thus others have argued that beta functions to promote tonic motor activity at the expense of voluntary movement (Engel and Fries, 2010; Jenkinson and Brown, 2011). Cortical beta is likely to be partially generated via interactions with the basal ganglia and is enhanced in Parkinson's disease (Jenkinson and Brown, 2011). Beta may also be produced by cortico-cortical and even cortico-spinal interactions. Indeed, modeling studies suggest that beta oscillations are ideally suited for communicating across long conduction delays (Bibbig et al., 2002; Kopell et al., 2000).

In scalp recordings, theta is most prominently seen over frontal midline locations (Maurer and Dierks, 1991; Mitchell et al., 2008; Nunez et al., 2001; Srinivasan et al., 2006) and has been found to be modulated by multiple cognitive demands such as working memory (Onton et al., 2005) and error monitoring (Debener et al., 2005). This "frontal-midline" theta is consistent with generators in the anterior cingulate (Onton et al., 2005), and correlates with simultaneously recorded BOLD activity in this area (Debener et al., 2005). Intracranial recordings have confirmed feedback related theta activity in the anterior cingulate (Wang, 2005), but they have also revealed theta activity in many other cortical areas. Theta has been associated with the temporal lobe in human intracranial recordings (Sperling, 1993), though various tasks (navigation, speech comprehension, working memory) have been shown to modulate theta in occipital, frontal, pericentral, and orbitofrontal areas (Canolty et al., 2006; Kahana et al., 1999; Raghavachari, 2006). Many non-mutually exclusive, functions for cortical theta oscillations have been proposed such as executive attention (Wang, 2005), mediating communicating between different cortical areas by modulating local levels of activity (Canolty et al., 2006), mediating interactions with the hippocampus (Mitchell et al., 2008), working memory maintenance (Raghavachari, 2006), and spike-phase encoding (Wang, 2010).

The other conventional frequency bands are not clearly associated with particular cortical areas. In healthy adults, delta power is broadly distributed at the scalp, being largest over frontal and medial centroparietal sites (Maurer and Dierks, 1991). Gamma and high gamma modulations by tasks or the phase of low frequency oscillations have been demonstrated across multiple cortical areas (Canolty et al., 2006; Crone et al., 2011; Miller et al., 2012; Voytek, 2010). However, it is likely that these modulations reflect broadband changes in the

magnitude of the 1/*f* distribution of spectral power rather than changes in the magnitude of oscillatory activity (Miller et al., 2009). Indeed, regions exhibiting particularly elevated levels of intrinsic gamma or high gamma activity (indicative of true oscillations) have not been established, though there is some evidence of gamma/high gamma activity in medial temporal cortical areas during both wake and sleep states (Uchida et al., 2001).

Outstanding questions

While a small number of cortical regions have been identified that robustly exhibit intrinsic oscillations in particular frequency ranges, it is not clear what type of intrinsic oscillatory activity is normally present for the majority of regions. For example, based on high-density EEG and MEG recordings, Nunez et al. (2001) and Srinivasan et al. (2006) have argued that alpha activity dominates the intrinsic activity of cortex in general, although some areas (e.g., occipital) exhibit more alpha power than others. However alpha activity is not reported as being that widespread in contemporary neurological intracranial EEG atlases (Sperling, 1993, 2003). Similarly, although beta is clearly characteristic of sensorimotor cortex, it is not clear how far it extends beyond those areas. There are reports of intrinsic beta oscillations being found over other areas of the frontal lobe (Penfield and Jasper, 1954; Sperling, 1993) as well as the medial temporal lobe (Uchida et al., 2001). Developing a more comprehensive atlas of the types of oscillatory activity that are normally generated by different cortical areas is of obvious clinical importance, since such standards should aid in the identification of pathological brain areas. Moreover, it would help with interpreting the growing body of research on resting state EEG/MEG data (Mantini et al., 2007) and inform our understanding of the role and networks involved in producing these oscillations.

An additional shortcoming of our current knowledge of intrinsic brain oscillations is the lack of a clear understanding as to what types of frequencies of oscillations exist. The conventional frequency bands are likely based on the few most robust examples of intrinsic oscillations (e.g., occipital alpha, mu) and may not be generally valid (Niedermeyer and da Silva, 1993). For example, the theta band was originally defined to characterize EEG abnormalities produced by tumors whose periods were in between that of prototypical delta and alpha phenomena (Walter and Dovey, 1944). Decades of subsequent research have found that various factors can modulate theta activity in healthy individuals but it is quite possible that multiple, distinct physiological processes produce theta band oscillations and that some theta band activity may be functionally and physiologically identical to oscillations outside of the theta band (Mitchell et al., 2008). Since such frequency band conventions are often applied a priori to determine the spectral resolution of analyses (Mantini et al., 2007), there is a clear need to demonstrate their validity.

The present research aims to address these questions by measuring intrinsic oscillations across a wide range of cortical areas utilizing ECoG data obtained from a relatively large sample of patients with pharmacoresistant epilepsy. The data were acquired while participants were in a resting state and electrodes exhibiting pathological activity or near structural abnormalities were removed from analysis in order to capture normal brain activity as best as possible. ECoG data were grouped across participants according to a surface based atlas of cortical areas, and peaks were analyzed according to conventional

frequency bands. In addition, cluster analysis was applied to these data to distinguish types of cortical oscillations without having to make a priori anatomical or frequency band groupings.

Materials and methods

Participants

ECoG data were provided by 15 individuals (6 males, mean/SD age = 32/13 years, 14 right handed, 1 left handed) with pharmacoresistant epilepsy undergoing intracranial EEG monitoring at the Hofstra North Shore-LIJ School of Medicine. All patients provided informed consent in accordance with the Declaration of Helsinki, as monitored by the local institutional review board. Low functioning patients and patients with grossly abnormal brains (e.g., significant prior resections or structural abnormalities) were excluded from participation. The decision to implant, the electrode targets, and the duration of implantation were determined entirely on clinical grounds without reference to this investigation. Fourteen participants received surgery following intracranial monitoring and, in all but one case, experienced at least some seizure relief (median/SIQR Engel outcome = 2.0/1.0), which suggests that abnormal brain areas were at least partially identified. The median time between surgery and the last clinical follow up with each patient is 13.5 months (SIQR = 4.5).

ECoG data collection and spectral analysis

ECoG data were recorded using Adtech platinum 3 mm diameter electrodes and an Xltek EMU 128 clinical recording system. Sampling rate varied from 500 to 2000 Hz using an analog bandpass filter with half-power boundaries of 0.07 Hz and 40% of the sampling rate (e.g., 200 Hz upper cut off when recording at 500 Hz). Data recorded at 2000 Hz (two participants) were downsampled to 1000 Hz to ease computational demands using the MATLAB function *decimate* and a 30th order antialiasing FIR filter (MATLAB 7.9, The MathWorks Inc., Natick, MA, 2009). ECoG channels were recorded relative to a reference electrode screwed into the vertex of the skull. On average, 103 (SD = 21) electrodes were implanted per participant. A board certified neurologist identified electrodes over the ictal onset zone and near anatomical abnormalities (e.g., tumor, dysplasia). These electrodes as well as electrodes over non-neocortical areas (e.g., amygdala), contaminated by frequent interictal spikes or drift, or with poor signal-to-noise were rejected from analysis. This left an average of 81 (SD = 26) channels per participant. These remaining channels were converted to the average reference to minimize line noise.

Data were acquired when an experimenter asked the participant to lie still with her/his eyes closed for 3 to 7 min (10 participants) or from archived data based on simultaneously recorded video while patients appeared to be in resting wakefulness with eyes closed (five participants). For the archived data, five to six minute periods of time were found when the patient was awake but resting, and occasional periods of movement in these data were noted and removed from analysis. On average, each participant provided 4.75 (SD = 1.36) minutes of data for analysis. All but one participant was on some type of antiepileptic medication at

the time of data acquisition, though sometimes at tapered doses. All data were acquired at least 17 h since the last clinical seizure.

The spectral power density (SPD) for each channel was estimated using a one second moving window (0.5 s steps) and the discrete Fourier transform (DFT) with two Slepian tapers (Kleinfeld and Mitra, 2011) using the Chronux MATLAB toolbox (Bokil et al., 2010). This provides a frequency resolution of 1 Hz and a frequency resolution bandwidth of 3 Hz. Prior to the DFT the mean of each one second window was removed to dampen low frequency activity (e.g., drift). SPD estimates from each one second window were averaged using the 20% trimmed mean (Wilcox, 2003), so that averages were robust to occasional outliers. The SPD for each channel was estimated both for the raw data and for temporally whitened data. Temporal whitening simply consists of subtracting the value of each time point from that of the immediately subsequent time point (Kleinfeld and Mitra, 2011). This procedure dampens the 1/f tendency in the ECoG power spectra and makes SPD peaks more salient (Fig. 1).

To control for differences in overall power across channels and participants, the average SPD at each channel was normalized to unit power across frequencies of interest: 1–51, 64–116, and 124–161 Hz. These frequency bands were chosen to avoid 60/120 Hz line noise and because non-artifactual SPD peaks were not observed above 161 Hz.

Electrode localization

To identify the electrode locations, all participants received an anatomical T1-weighted MRI before electrode implantation as well as a full head CT scan and an anatomical T1-weighted MRI after electrode implantation. Preimplant MRIs were performed on a General Electric Signa HDx 3-T scanner using one of two spoiled gradient recalled sequences [FOV = 256 or 240 mm, voxel size 1 × 1 × 1 or 1.2 × 0.9 × 0.9, matrix 256 × 256, flip angle = 8, TR = 7.8 or 6.5 ms, TE = 3.0 or 2.8, TI = 650 or 600 ms, acquisition plane = axial or sagittal, slices = 180 or 170]. Postimplantation volumetric MRIs were performed on a 1.5 T scanner using standard clinical protocols.

Electrode locations were manually identified on the CT scan using the software BioImage Suite (Version 3, http://www.bioimagesuite.org). These locations were then mapped to the preimplant MRI via an affine transformation derived from coregistering the preimplant and postimplant MRIs and postimplant MRI and CT scans using FLIRT (Jenkinson and Smith, 2001) and the skull-stripping BET algorithm (Smith, 2002), both part of the Oxford Centre for Functional MRI of the Brain (FMRIB) software library (FSL: www.fmrib.ox.ac.uk/fsl). The reconstructed pial surface was computed from the preimplant MRI using FreeSurfer (http://surfer.nmr.mgh.harvard.edu/) and the electrode coordinates projected to the pial surface (Dykstra et al., 2011) to correct for possible brain shift caused by electrode implantation and surgery. Intraoperative photographs and electrical stimulation mapping were used to corroborate this registration method. This pial surface projection method has been shown to produce results that are quite compatible with the electrode locations in intraoperative photographs (median disagreement of ~3 mm, Dykstra et al., 2011).

Once electrode locations were projected to the pial surface, each electrode was assigned to one of 35 cortical areas (Figs. 1 & 4) using the Desikan-Killiany atlas (Desikan et al., 2006). For visualizing electrode locations across participants, electrode locations were mapped to the FreeSurfer average brain (Fig. 7) using FreeSurfer's surface based co-registration (Fischl et al., 1999).

Cluster analysis

To identify types of SPDs, *k*-means cluster analysis was applied to the 1208 normalized SPDs from all channels. Each SPD was represented as a 142 dimensional vector, with each dimension corresponding to a different frequency (1–51, 64–116, & 124–161 Hz at 1 Hz steps). As mentioned previously, each vector was normalized such that all the elements of a vector summed to one. SPD was in units of (μV^2)/Hz prior to normalization. The Euclidean distance between each normalized SPD was used as the measure of SPD dissimilarity for clustering.

Stability-based validation (Lange et al., 2004) was used to determine the number of latent clusters in the data. Specifically, to determine the relative stability of a specific number of clusters *k*, the following process was repeated 800 times:

1. The 1208 SPDs were randomly split into two equal groups: Group A and Group B
2. Each of the two groups was independently clustered using *k*-means and *k* clusters. For each group, the cluster analysis was repeated 50 times using different initial centroids (*k* randomly selected data points). The best solution of the 50 trials was used.
3. Each SPD in Group B was assigned to a cluster in Group A based on its distance to Group A's cluster centroids. The amount of disagreement between the cluster solutions produced by both groups was then calculated.
4. The disagreement between cluster solutions is normalized by the amount of disagreement one would achieve from randomly assigning SPDs to clusters since with fewer clusters greater agreementis expected by chance. This normalization value was estimated by repeating steps 1–3 200 times and randomly permutating the cluster assignments in Group B before measuring split-half disagreement.

The disagreement from each of the 200 splits of the data was averaged (Fig. 5). Local minima in disagreement correspond to relatively stable solutions. For these local minima, the *k*-means process was repeated using the full set of SPDs 100 times using different initial centroids (*k* randomly selected data points). The best of the 100 solutions was taken as the final solution.

Results

Most commonly observed spectral power peaks

For each channel, frequencies exhibiting whitened SPD peaks were identified as those with greater power than the immediately preceding and subsequent frequencies (e.g., Fig. 1: Right). Fig. 2 shows the preponderance of peaks across frequencies of interest. This method

was generally effective at capturing peaks for frequencies below 40 Hz, due to the residual 1/*f* trend in the SPD. However, as the SPDs tend to flatten at higher frequencies, small deviations in power often qualified as peaks even though they are likely not reliable. In the sub-40 Hz range, peaks are most commonly seen around 7 Hz with less frequent modes at 3, 9, 15, 22, and possibly 35 Hz.

Cortical area average SPDs

Electrodes were grouped according to cortical area and their SPD averaged within participant and then across participants (i.e., the mean from each participant was weighted equally). Fig. 3 shows these averages both for nonwhitened and whitened SPDs (see also Supplemental Figs. 1 & 2). As with the prior analysis of peak frequencies (see previous section), theta peaks are prominent in several areas while alpha peaks are rare, seen only in lateral occipital cortex and, possibly, the pars opercularis. Beta peaks are seen in several areas, most clearly in the pre- and postcentral gyri. Tendencies for gamma/high gamma peaks (Supplemental Fig. 3) were also found over several temporal areas (entorhinal cortex, parahippocampal gyrus, temporal pole) and some frontal areas (orbitofrontal cortex, frontal pole). Since all of these tendencies are also observed in the nonwhitened data, they are clearly not an artifact of the whitening.

To determine how reliable these peaks are across individuals, the mean peak frequency across participants was estimated for each area in three frequency ranges based on conventional boundaries: 1–12 Hz (delta, theta, & alpha), 13–30 Hz (beta), and 31–127 Hz (gamma/high gamma). Data for each participant were weighted equally (despite individual variation in the number of electrodes in each area). Thus the degrees of freedom for each estimate is the number of participants contributing data to each area minus one. Estimates were made for the 23 cortical areas from which more than three participants contributed data. Areas with data from three or fewer participants were excluded as their estimates would be likely unreliable and including them would hurt statistical power at others. Two-tailed, one sample *t*-tests were used to evaluate how reliably mean peak frequency differed from that of conventional boundaries in the 1–12 Hz band. Upper-tailed, one sample *t*-tests were used for beta and gamma bands and the peaks in these bands were log transformed to make their positively skewed distributions more normal (Zar, 1999). The Benjamini-Hochberg false discovery rate (FDR) control algorithm (Benjamini and Hochberg, 1995) was used to adjust *p*-values for each family of 23 hypothesis tests.

In the lowest frequency band, mean peak frequency tended to be around the border of theta and alpha (Fig. 4: A). Indeed, the mean peak across all areas in this band was 7.0 Hz (SE: 0.7 Hz), which is significantly below the 10 Hz peak frequency typically seen at the scalp ($t(14) = -4.09$, $p = 0.001$). Save for the frontal pole, pars orbitalis, entorhinal cortex, and the parahippocampal gyrus, the mean peak frequency of areas was reliably above the delta band. No areas reliably showed peaks in the alpha band though the superior frontal gyrus, temporal pole, middle temporal gyrus, and entorhinal cortex tended to peak below alpha ($p_{adj} > 0.05$). Beta band peaks appeared reliably over the precentral, postcentral, rostral middle frontal, and caudal middle frontal gyri, as well as over the pars opercularis (Fig. 4: B). No areas showed reliable gamma peaks ($p_{adj} > 0.18$) though some channels with clear

gamma peaks were occasionally found. These tended to be in the anterior temporal lobe, especially over entorhinal and parahippocampal areas (Fig. 4: C).

Given the substantial individual variability in mean peak frequency, we looked to see if patient age or the circumstances in which the data were acquired could explain some of this variation using ordinary least squares linear regression. The regression model consisted of two predictors, an intercept, and a Gaussian noise term. The predictor representing the circumstances of data acquisition was coded as 1 if the data were acquired in a controlled manner and 0 if the data were extracted based on archived video. The analysis was applied independently to each of the 23 cortical areas with sufficient data and Benjamini-Hochberg FDR control was used to adjust *p*-values for each family of 23 tests. Again, peaks in the beta and gamma bands were log transformed to make their positively skewed distributions more normal. Estimated effects of age are presented in Supplemental Fig. 4. There was a general tendency for peak frequency to increase with age that approached significance in the 1–12 Hz band over the superior frontal, rostral middle frontal, medial orbitofrontal, and middle temporal gyri ($p_{adj} = 0.06$). In the other frequency bands, no effects were reliable ($p_{adj} > 0.62$). In contrast, the regression analysis found no evidence that peak frequency differed between data sets that were acquired in a controlled setting and those taken from archived video ($p_{adj} > 0.18$, Supplemental Fig. 5).

Cluster analysis

Two clusters proved to be the most reliable way of grouping the SPDs from all 1208 channels (Fig. 5). The two cluster solution grouped together SPDs with delta and theta peaks separately from those with alpha and beta peaks (Fig. 6: A). There is a tendency for the higher frequency cluster to predominate pericentral, occipital, parietal areas and the lower to dominate the temporal and frontal lobes (Supplemental Fig. 6).

A clear local minima at seven clusters (Fig. 5) revealed a grouping of SPDs that was similar to conventional frequency band delineations (Fig. 6: B). The centroids of three of the seven clusters exhibited peaks at 3 (delta), 10 (alpha), and 17 (beta) Hz. Three other clusters fell within the theta band with centroid peaks at 5 and 7 Hz. The centroid of the final cluster was broadly distributed with slight peaks at 8, 19, and 42 Hz. Figs. 7, 8, and Supplemental Fig. 7 show the distribution of cluster members across cortex. The delta cluster appears most clearly in frontal areas (especially the frontal pole), but also in superior temporal and inferior parietal regions. The 5 Hz cluster appears predominantly in frontal and temporal regions, though also in the posterior cingulate and precuneus where few participants had electrodes. The narrow band 7 Hz cluster appeared relatively frequently in parietal and temporal areas, whereas the broader 7 Hz cluster was predominantly in occipital and inferior temporal areas (though also in the frontal pole). The 10 Hz cluster was the most common type of SPD in occipital and parietal areas. The 17 Hz cluster was clearly predominant over the pericentral gryi and was also relatively common in the middle frontal gyrus and pars opercularis. Finally, the broadly distributed 8, 19, and 42 Hz cluster tended to occur most frequently over orbitofrontal and medial temporal regions.

Discussion

Types and anatomical foci of oscillations in the human electrocorticogram

In the early years of human electrophysiology, it was thought that cytoarchitectonically distinct cortical regions would exhibit distinct patterns of intrinsic electric activity (Penfield and Jasper, 1954). However, this soon appeared not to be the case as expert visual inspection of spontaneous iEEG/EEG recordings identified only a handful of rhythms with a relatively crude degree of anatomical specificity (Ibid). With the recent significant advances in the development of human brain atlases, our ability to identify the location of intracranial electrodes relative to such atlases, and our tools for processing and identifying complex patterns in large amounts of electrophysiological data, we believe that the intrinsic electrical activity of the brain will prove to be much more anatomically differentiated and useful for identifying functional and diseased brain networks.

The present study is a step in this direction. Specifically, our goal was to characterize the types of oscillations apparent in the human electrocorticogram and the predominance of these oscillations in different cortical areas using a surface based cortical atlas as well as anatomically agnostic cluster analyses. Our results confirmed the presence of two of the most robustly observed rhythms: pericentral beta (MacKay, 1997) and occipital–parietal alpha (Perez-Borja et al., 1962; Sperling, 1993). In addition, evidence of theta oscillations was observed over superior frontal cortex, a location consistent with frontal midline theta activity found in EEG and MEG (Mitchell et al., 2008). The anterior cingulate is another putative source of frontal midline theta (Debener et al., 2005; Onton et al., 2005), but because only one participant had electrodes over the anterior cingulate, we could not assess the reliability of activity there. Surprisingly, pericentral mu (Sperling, 1993) was not robustly observed in these data. Although clear mu peaks were observed over the pre- and postcentral gyri in some channels, theta and beta peaks were more dominant in others, which masked the mu peaks in the group analyses. We suspect that mu activity would be more pronounced if we used a finer grained cortical atlas that parcellated pericentral cortex into more than just two areas (pre- and postcentral gyri).

In addition to confirming those expected rhythms, several novel results were obtained. In particular, the most dominant oscillation seen throughout the cortical areas sampled tended to be around 7 Hz. This was apparent in both the whitened and unwhitened SPDs when grouping electrodes by cortical area and also in the peak histograms and cluster analysis of the whitened SPDs. This is a surprising result given that ~10 Hz activity is generally the most prominent SPD peak at the scalp (Maurer and Dierks, 1991; Nunez et al., 1978, 2001), and that attempts to localize eyes closed high-density EEG and MEG data have suggested that alpha should be the most dominant frequency across much of cortex (Nunez et al., 2001; Srinivasan et al., 2006). However, the result is quite clear in these data and appear to be corroborated by a previous, smaller ECoG study by Voytek (2010) that analyzed ECoG data from two patients performing a variety of visual, auditory, and/or motor tasks. Their study found that theta power was generally stronger than alpha across all the areas sampled (occipital, temporal, and parietal sites were sampled in both patients). The propenderance of theta supports theories that posit a very general role for theta in cortical processing, such as

mediating communication between cortical areas (Canolty et al., 2006), top-down processing (Kahana et al., 2001), and learning and memory (Mitchell et al., 2008; Raghavachari, 2006; Wang, 2010). In contrast, alpha activity was generally limited to the occipital and parietal lobes, which suggests a more limited role in cortical processing than has been proposed previously (Nunez et al., 2001). In particular, alpha may primarily be involved in some aspects of sensory processing and attention (Jensen and Mazaheri, 2010; Klimesch et al., 2007; Voytek, 2010).

It is not clear why theta activity is much more prominent in ECoG recordings than in EEG/MEG. It may be that alpha volume conducts to the scalp better than theta because alpha's magnitude is greater or alpha is more phase coherent across areas. In addition, clinicians have observed that drowsiness enhances EEG theta power and diminishes alpha oscillations (Niedermeyer and da Silva, 1993) and some of our participants may have been in a fatigued state due to the potential discomfort of multi-day intracranial EEG monitoring. However, it is not clear how strong an effect drowsiness has on the peak frequencies of intracranial EEG and there is some evidence from experimental studies that fatigue can produce broadband increases in EEG power as well (especially in the alpha and beta bands, Huang et al., 2008). Finally, since almost all participants were on antiepileptic drugs (AEDs) at the time of data acquisition, it is possible that they are at least partially responsible for the predominance of theta activity as AEDs tend to enhance EEG theta power (Blume, 2006) and to enhance lower frequencies (e.g., delta and theta) relative to higher frequencies in iEEG (Zaveri et al., 2010). Nonetheless, the effect of AEDs appears to be quite small at the scalp (~4% at occipital electrodes–Salinsky et al., 2002, 2003, 2007) and it is not clear how large the differential effect of AEDs on intracranial theta and alpha is (Zaveri et al., 2010). Consequently, we think AEDs alone are unlikely to explain the clear predominance of theta in our data. Replicating this study using simultaneous ECoG and EEG recordings and controlling for medications should help determine the extent to which volume conduction and drug effects can explain why theta is much more prevalent in intracranial than scalp EEG.

Another novel result involving theta, was the evidence of two subbands of theta activity, 5 and 7 Hz, found by the cluster analysis. The channels displaying increased 5 Hz activity appeared predominantly in the frontal and temporal regions, and in the posterior cingulate and precuneus in the few participants who had electrodes there. Channels showing predominantly 7 Hz activity appeared relatively frequently in the occipital, temporal, and parietal lobes, and also over the frontal pole. Although multiple, dissociable mechanisms for theta are likely to exist (Mitchell et al., 2008), to the best of our knowledge, different low and high theta sub-bands have not been established. Given that much research on ECoG oscillations is based on time-frequency analysis with relatively crude frequency resolution, distinct theta sub-bands may exist but be typically blurred together in analyses. Alternatively, the distinct clusters may reflect more individual differences in theta peak frequency than functional differences. Thus further work is needed to establish if these sub-bands are indeed meaningful.

Below these frequencies, in the delta band, we found several channels with clear ~3 Hz peaks. These channels tended to be in frontal areas (especially the frontal pole), but also

were found in superior temporal and inferior parietal regions. The predominance of intracranial 3 Hz activity in the frontal lobes appears consistent with the relatively high delta power typically found across frontal scalp regions (Maurer and Dierks, 1991). Note that it is likely that the preponderance of delta activity is underestimated and its central frequency distorted in our results because we high-pass filtered the data (whitening and removal of the DC component of each one second epoch) prior to estimating SPDs. Alternative data preprocessing might better capture delta band activity.

In addition to confirming the pericentral dominance of beta activity, we also found pronounced beta activity in other frontal regions. Although beta activity has been described as being generally characteristic of the frontal lobe (Sperling, 1993), we found that it was particularly prominent in the middle frontal gyrus (both rostrally and caudally) and the pars opercularis. Tendencies for beta activity were also observed over the lateral orbitofrontal gyrus and entorhinal cortex, but not as consistently. Given that Uchida et al. (2001) found beta activity over the medial temporal lobe, we believe that entorhinal beta is reliable, though not as pronounced as it is in frontal areas. Frontal beta may simply reflect its role in areas involving motor networks (Fesl and Yousry, 2007; Jenkinson and Brown, 2011; MacKay, 1997). However, beta activity in these regions has also been associated with other cognitive functions such as speech comprehension (Canolty et al., 2007), visual perception (Sehatpour et al., 2008), and executive functions (Buschman et al., 2012). Thus this activity may reflect a more general role for beta in mediating long distance communication between these areas and other brain regions (Bibbig et al., 2002; Kopell et al., 2000), language processing (Canolty et al., 2007), or maintaining cognitive states (Engel and Fries, 2010). With regard to entorhinal beta, Uchida et al. (2001) have speculated that it is the human analog of “rhythmic slow activity” in animal models of memory and involved in memory consolidation.

With regard to the gamma and high gamma bands, peaks in these ranges were observed in some electrodes but this activity was not pronounced enough and varied too much across participants to be reliably characterized. When gamma peaks were present, they tended to be in the temporal lobe, especially over anterior and medial regions. There was evidence for gamma activity in the orbitofrontal cortex as well. Uchida et al. (2001) previously reported gamma peaks in the intrinsic activity of the medial temporal lobe. However, it is not clear from their analyses if these peaks were reliably observed across participants, and they note that the anatomical focus of this activity varied across individuals. Thus their results may be compatible with ours. Part of the difficulty with attempting to characterize gamma activity is that gamma power is relatively weak even after whitening the data to dampen the $1/f$ SPD trend. Alternative filtering could enhance the ability to detect and characterize gamma.

Finally, we note that while some cortical areas did exhibit reliable peaks in spectral power that differentiated them from other areas, in general there was substantial variability in the dominant frequencies within each region. This suggests a low degree of regional specificity for oscillations across the cortical parcellations used here. There are several reasons why we are likely underestimating the degree of regional specificity. We suspect that individual differences in patient state and characteristics could account for a lot of this variability. We found a borderline significant trend for peak frequency in the 1–12 Hz range to increase with

age over several frontal areas and the middle temporal gyrus. This would be consistent with evidence of a decrease in EEG theta and delta power relative to alpha power observed with increasing age (Dustman et al., 1999). We did not find any evidence of systematic differences in spectral peaks between data collected in a controlled setting and those gathered from archived data based on video of the patients. However, even though care was taken to make sure patients were alert and immobile during data collection, there may have been significant differences in the state of alertness and restedness across patients that would affect our results (Niedermeyer and da Silva, 1993). Moreover, differences in medication and patient etiology may have systematically influenced dominant frequencies to some extent as well.

Shortcomings of the Desikan-Killiany cortical parcellation used to define areas and the fact that several analyses combined electrodes across hemispheres may also have contributed to the high within-area variability in dominant frequencies. The anatomically agnostic cluster analysis (Fig. 7) suggests that a finer grained cortical parcellation than the 35 area Desikan-Killiany atlas might provide somewhat greater anatomical specificity. However, there is still a considerable amount of local heterogeneity in the types of spectral peaks found by the cluster analysis, suggesting that the degree of improvement would be small. Alternatively, it may be that the pattern of gyrification, on which our cortical parcellation is based, is a poor match to oscillatory networks and that functionally defined areas (e.g., Craddock et al., 2011; Power et al., 2011) might better identify homologous areas across individuals with more similar oscillatory dynamics.

Limitations of methods & future work

The greatest limitation of this study is that the data were all acquired from individuals with pharmacologically intractable epilepsy undergoing invasive intracranial EEG monitoring for a period of several days. Consequently, it is possible that the data are not very representative of normal brain activity. Although we excluded patients with extensive brain abnormalities and specific electrodes exhibiting epileptiform activity or near structural abnormalities, it is still possible that the data may be confounded due to factors such as brain reorganization, medications, the influence of abnormal areas on the regions included in our analysis, pathological areas mis-diagnosed as healthy and included in our analysis, and the possible effects of intracranial monitoring. Our results, however, are corroborated in many ways by non-invasive measures in healthy adults and invasive animal recordings. Moreover, EEG effects of AEDs appear to be rather limited (Blume, 2006; Salinsky et al., 2002, 2003, 2007). Future work using animal models or simultaneous ECoG and non-invasive measures should provide a better sense of how representative these results are of normal human brain activity. Moreover, in the future, we hope to compare ECoG oscillations as patient medications are varied during the course of their observation (e.g., Zaveri et al., 2010). This should give us a clearer sense of how antiepileptic and analgesic medications might have affected these results.

Another limitation of this study is the anatomical sampling bias of ECoG recordings. The number of ECoG electrodes is necessarily restricted and they are placed only over the gyri of suspected pathological areas or adjacent eloquent cortex. In these data, we have frequent

coverage of much of the lateral surfaces of the frontal, parietal, and temporal lobes. However, there are few medial or occipital lobe electrodes, and we combined electrodes from both hemispheres for some analyses to maximize the number of participants contributing data to each cortical area. These shortcomings could have biased our analyses because the coverage within a cortical area was not uniform, because some areas contributed disproportionally to the clustering results, and because there may be some significant hemispheric asymmetries in intrinsic oscillations (Srinivasan et al., 2006). For example, alpha activity surely would have been more prominent in our data had we had greater coverage of occipital areas (Perez-Borja et al., 1962). However, given that we were able to record from most cortical areas in several participants and captured many expected oscillatory phenomena (including posterior alpha), we do not think this bias is severe. Hopefully, advances in ECoG technology (Viventi et al., 2011), developing larger databases of ECoG data like these (www.ieeg.org), and animal models will allow more comprehensive, detailed, and uniform sampling of cortical activity in the near future that will mitigate this issue.

Note that although these methodological limitations complicate making generalizations about normal brain function, they do not limit the potential clinical utility of these data since they should be representative of ECoG data collected from nonepileptiform cortical areas of individuals with pharmacologically intractable epilepsy. Some abnormalities in intrinsic brain oscillations have been previously identified that are indicative of pathological areas. For example, structural abnormalities (e.g., gliosis) can cause focal attentuation of alpha and beta activity (Sperling, 2003) and there is growing evidenct that extremely high frequency oscillations are indicative of epileptogenic cortex (Bragin et al., 2010). We suspect that the intrinsic oscillatory activity of epileptogenic cortical areas will likely significantly deviate from that of nonepileptogenic areas in ways that have escaped notice due to the lack of quantitative norms. In future work, we plan to determine if this is indeed the case and encourage others to also collect resting state data like those we have analyzed here to help establish such norms (similar to what is being attempted with fMRI for the diagnosis of brain disorders–Biswal et al., 2010).

Conclusions

Our analysis of intrinsic activity across a large number of human cortical areas found distinct frequencies of oscillations that are particularly likely to occur. Although the types of oscillations most prominent in a particular cortical area were generally quite variable, some frequencies of oscillations proved to be characteristic of a few specific cortical areas. Cluster analysis suggests seven typical types of oscillations. Six of these have peaks at 3, 5, 7 (narrow), 7 (broad), 10, and 17 Hz, while the remaining cluster is broadly distributed with less pronounced peaks at 8, 19, and 42 Hz. These categories largely corroborate conventional sub-gamma frequency band distinctions (delta, theta, alpha, and beta), and suggest multiple sub-types of theta. Of these types, the most prominent frequency of oscillation observed was around 7 Hz, which is significantly lower than the 10 Hz activity that dominates the intrinsic activity apparent in EEG/MEG recordings. Seven Hz activity was found widely throughout the brain (though was particularly prominent over some temporal and parietal regions). Prominent 10 Hz activity was found as well, but this was

largely limited to occipital and parietal regions where it likely serves a role in sensory processing and attention. As expected, 17 Hz activity was found prominently over pre- and post-central gyri. It was also pronounced over the middle frontal gyrus and pars opercularis, which may reflect the role of these area sinmotor networks, language processing, and executive functions. Three Hz, delta band peaks were found in several channels and tended to occur in frontal areas (especially the frontal pole), but also were found in superior temporal and inferior parietal regions. Finally, gamma/high gamma activity (+30 Hz) was sometimes prominently observed but was too infrequent and variable across individuals to be reliably characterized.

Supplementary Material

Refer to Web version on PubMed Central for supplementary material.

Acknowledgments

The authors would like to thank David Kleinfeld for advice on spectral analysis, Connor Garret for help in collecting some of the data, and three anonymous reviews for their feedback on an earlier version of this manuscript. This work was supported by the Page & Otto Marx Jr. Foundation, the National Institute of Neurological Disorders and Stroke (F31NS080357-01 and T32-GM007288), and the Epilepsy Foundation of America (EFA189045).

References

Benjamini Y, Hochberg Y. Controlling the false discovery rate: a practical and powerful approach to multiple testing. J R Stat Soc Ser B Methodol. 1995; 57:289–300.

Bibbig A, Traub RD, Whittington MA. Long-range synchronization of γ and β oscillations and the plasticity of excitatory and inhibitory synapses: a network model. J Neurophysiol. 2002; 88:1634–1654. [PubMed: 12364494]

Biswal BB, Mennes M, Zuo XN, Gohel S, Kelly C, Smith SM, Beckmann CF, Adelstein JS, Buckner RL, Colcombe S, Dogonowski AM, Ernst M, Fair D, Hampson M, Hoptman MJ, Hyde JS, Kiviniemi VJ, Kotter R, Li SJ, Lin CP, Lowe MJ, Mackay C, Madden DJ, Madsen KH, Margulies DS, Mayberg HS, McMahon K, Monk CS, Mostofsky SH, Nagel BJ, Pekar JJ, Peltier SJ, Petersen SE, Riedl V, Rombouts SARB, Rypma B, Schlaggar BL, Schmidt S, Seidler RD, Siegle GJ, Sorg C, Teng GJ, Veijola J, Villringer A, Walter M, Wang L, Weng XC, Whitfield-Gabrieli S, Williamson P, Windischberger C, Zang YF, Zhang HY, Castellanos FX, Milham MP. Toward discovery science of human brain function. Proc Natl Acad Sci. 2010; 107:4734–4739. [PubMed: 20176931]

Blume WT. Drug effects on EEG. J Clin Neurophysiol. 2006; 23:306. [PubMed: 16885705]

Bokil H, Andrews P, Kulkarni JE, Mehta S, Mitra PP. Chronux: a platform for analyzing neural signals. J Neurosci Methods. 2010; 192:146–151. [PubMed: 20637804]

Bragin A, Engel J Jr, Staba RJ. High-frequency oscillations in epileptic brain. Curr Opin Neurol. 2010; 23:151–156. [PubMed: 20160649]

Buschman TJ, Denovellis EL, Diogo C, Bullock D, Miller EK. Synchronous oscillatory neural ensembles for rules in the prefrontal cortex. Neuron. 2012; 76(4):838–846. http://dx.doi.org/10.1016/j.neuron.2012.09.029. [PubMed: 23177967]

Canolty RT, Edwards E, Dalal SS, Soltani M, Nagarajan SS, Kirsch HE, Berger MS, Barbaro NM, Knight RT. High gamma power is phase-locked to theta oscillations in human neocortex. Science. 2006; 313:1626–1628. [PubMed: 16973878]

Canolty RT, Soltani M, Dalal SS, Edwards E, Dronkers NF, Nagarajan SS, Kirsch HE, Barbaro NM, Knight RT. Spatiotemporal dynamics of word processing in the human brain. Front Neurosci. 2007; 1:185. [PubMed: 18982128]

Craddock RC, James GA, Holtzheimer PE III, Hu XP, Mayberg HS. A whole brain fMRI atlas generated via spatially constrained spectral clustering. Hum Brain Mapp. 2011; 33(8):1914–1928. http://dx.doi.org/10.1002/hbm.21333. [PubMed: 21769991]

Crone NE, Korzeniewska A, Franaszczuk PJ. Cortical gamma responses: searching high and low. Int J Psychophysiol. 2011; 79:9–15. [PubMed: 21081143]

Debener S, Ullsperger M, Siegel M, Fiehler K, Von Cramon DY, Engel AK. Trial-by-trial coupling of concurrent electroencephalogram and functional magnetic resonance imaging identifies the dynamics of performance monitoring. J Neurosci. 2005; 25:11730–11737. [PubMed: 16354931]

Desikan RS, Ségonne F, Fischl B, Quinn BT, Dickerson BC, Blacker D, Buckner RL, Dale AM, Maguire RP, Hyman BT, Albert MS, Killiany RJ. An automated labeling system for subdividing the human cerebral cortex on MRI scans into gyral based regions of interest. NeuroImage. 2006; 31:968–980. [PubMed: 16530430]

Dustman RE, Shearer DE, Emmerson RY. Life-span changes in EEG spectral amplitude, amplitude variability and mean frequency. Clin Neurophysiol. 1999; 110:1399–1409. [PubMed: 10454276]

Dykstra AR, Chan AM, Quinn BT, Zepeda R, Keller CJ, Cormier J, Madsen JR, Eskandar EN, Cash SS. Individualized localization and cortical surface-based registration of intracranial electrodes. NeuroImage. 2011:1–42.

Engel AK, Fries P. Beta-band oscillations —signalling the status quo? Curr Opin Neurobiol. 2010; 20:156–165. [PubMed: 20359884]

Feige B. Cortical and subcortical correlates of electroencephalographic alpha rhythm modulation. J Neurophysiol. 2005; 93:2864–2872. [PubMed: 15601739]

Fesl G, Yousry TA. Preoperative assessment: motor function. Clinical Applications of Functional Brain MRI. 2007

Fischl B, Sereno MI, Tootell RBH, Dale AM. High-resolution intersubject averaging and a coordinate system for the cortical surface. Hum Brain Mapp. 1999; 8:272–284. [PubMed: 10619420]

Fox MD, Greicius M. Clinical applications of resting state functional connectivity. Front Syst Neurosci. 2010; 4

Huang RS, Jung TP, Delorme A, Makeig S. Tonic and phasic electroenceph-alographic dynamics during continuous compensatory tracking. NeuroImage. 2008; 39:1896–1909. [PubMed: 18083601]

Jenkinson N, Brown P. New insights into the relationship between dopamine, beta oscillations and motor function. Trends Neurosci. 2011; 34:611–618. [PubMed: 22018805]

Jenkinson M, Smith S. A global optimisation method for robust affine registration of brain images. Med Image Anal. 2001; 5(2):143–156. http://dx.doi.org/10.1016/S1361-8415(01)00036-6. [PubMed: 11516708]

Jensen O, Mazaheri A. Shaping functional architecture by oscillatory alpha activity: gating by inhibition. Front Hum Neurosci. 2010; 4

Kahana MJ, Sekuler R, Caplan JB, Kirschen M, Madsen JR. Human theta oscillations exhibit task dependence during virtual maze navigation. Nature. 1999; 399:781–784. [PubMed: 10391243]

Kahana MJ, Seelig D, Madsen JR. Theta returns. Curr Opin Neurobiol. 2001; 11:739–744. [PubMed: 11741027]

Kelly C, Biswal BB, Craddock RC, Castellanos FX, Milham MP. Characterizing variation in the functional connectome: promise and pitfalls. Trends Cogn Sci. 2012; 16:181–188. [PubMed: 22341211]

Kleinfeld, D.; Mitra, PP. Spectral methods for functional brain imaging. In: Yuste, R., editor. Imaging: A Laboratory Manual (Book 1). Cold Spring Harbor Laboratory Press; New York: 2011. p. 143-158.

Klimesch W, Sauseng P, Hanslmayr S. EEG alpha oscillations: the inhibition-timing hypothesis. Brain Res Rev. 2007; 53:63–88. [PubMed: 16887192]

Kokkonen SM, Nikkinen J, Remes J, Kantola J, Starck T, Haapea M, Tuominen J, Tervonen O, Kiviniemi V. Preoperative localization of the sensorimotor area using independent component analysis of resting-state fMRI. Magn Reson Imaging. 2009; 27:733–740. [PubMed: 19110394]

Kopell N, Ermentrout GB, Whittington MA, Traub RD. Gamma rhythms and beta rhythms have different synchronization properties. Proc Natl Acad Sci. 2000; 97:1867. [PubMed: 10677548]

Kutas M, Dale A. Electrical and magnetic readings of mental functions. Cogn Neurosci. 1997:197–242.

Lange T, Roth V, Braun ML, Buhmann JM. Stability-based validation of clustering solutions. Neural Comput. 2004; 16:1299–1323. [PubMed: 15130251]

MacKay WA. Synchronized neuronal oscillations and their role in motor processes. Trends Cogn Sci. 1997; 1:176–183. [PubMed: 21223899]

Mantini D, Perrucci MG, Del Gratta C, Romani GL, Corbetta M. Electrophysiological signatures of resting state networks in the human brain. Proc Natl Acad Sci. 2007; 104:13170. [PubMed: 17670949]

Maurer, K.; Dierks, T. Atlas of Brain Mapping. Springer; 1991.

Miller KJ, Sorensen LB, Ojemann JG, den Nijs M. Power-law scaling in the brain surface electric potential. PLoS Comput Biol. 2009; 5:e1000609. [PubMed: 20019800]

Miller KJ, Hermes D, Honey CJ, Hebb AO, Ramsey NF, Knight RT, Ojemann JG, Fetz EE. Human motor cortical activity is selectively phase-entrained on underlying rhythms. PLoS Comput Biol. 2012; 8:e1002655. [PubMed: 22969416]

Mitchell DJ, McNaughton N, Flanagan D, Kirk IJ. Frontal-midline theta from the perspective of hippocampal “theta”. Prog Neurobiol. 2008; 86:156–185. [PubMed: 18824212]

Niedermeyer, E.; da Silva, FHL. Electroencephalography, Basic Principles, Clinical Applications, and Related Fields. 3. 1993.

Nunez PL, Reid L, Bickford RG. The relationship of head size to alpha frequency with implications to a brain wave model. Electroencephalogr Clin Neurophysiol. 1978; 44:344–352. [PubMed: 76540]

Nunez PL, Wingeier BM, Silberstein RB. Spatial-temporal structures of human alpha rhythms: theory, microcurrent sources, multiscale measurements, and global binding of local networks. Hum Brain Mapp. 2001; 13:125–164. [PubMed: 11376500]

Onton J, Delorme A, Makeig S. Frontal midline EEG dynamics during working memory. NeuroImage. 2005; 27:341–356. [PubMed: 15927487]

Penfield, W.; Jasper, HH. Epilepsy and the Functional Anatomy of the Human Brain. 1. Little, Brown; Boston: 1954.

Perez-Borja C, Chatrian GE, Tyce FA, Rivers MH. Electrographic patterns of the occipital lobe in man: a topographic study based on use of implanted electrodes. Electroencephalogr Clin Neurophysiol. 1962; 14:171–172. [PubMed: 14485320]

Power JD, Cohen AL, Nelson SM, Wig GS, Barnes KA, Church JA, Vogel AC, Laumann TO, Miezin FM, Schlaggar BL, Petersen SE. Functional network organization of the human brain. Neuron. 2011; 72:665–678. [PubMed: 22099467]

Raghavachari S. Theta oscillations in human cortex during a working-memory task: evidence for local generators. J Neurophysiol. 2006; 95:1630–1638. [PubMed: 16207788]

Raichle ME. The brain’s dark energy. Science. 2006; 314:1249. [PubMed: 17124311]

Ritter P, Moosmann M, Villringer A. Rolandic alpha and beta EEG rhythms’ strengths are inversely related to fMRI-BOLD signal in primary somatosensory and motor cortex. Hum Brain Mapp. 2009; 30:1168–1187. [PubMed: 18465747]

Rowe DL, Robinson PA, Rennie CJ. Estimation of neurophysiological parameters from the waking EEG using a biophysical model of brain dynamics. J Theor Biol. 2004; 231:413–433. [PubMed: 15501472]

Salinsky MC, Binder LM, Oken BS, Storzbach D, Aron CR, Dodrill CB. Effects of gabapentin and carbamazepine on the EEG and cognition in healthy volunteers. Epilepsia. 2002; 43:482–490. [PubMed: 12027908]

Salinsky MC, Oken BS, Storzbach D, Dodrill CB. Assessment of CNS effects of antiepileptic drugs by using quantitative EEG measures. Epilepsia. 2003; 44:1042–1050. [PubMed: 12887435]

Salinsky M, Storzbach D, Oken B, Spencer D. Topiramate effects on the EEG and alertness in healthy volunteers: a different profile of antiepileptic drug neurotoxicity. Epilepsy Behav. 2007; 10:463–469. [PubMed: 17337249]

Sehatpour P, Molholm S, Schwartz TH, Mahoney JR, Mehta AD, Javitt DC, Stanton PK, Foxe JJ. A human intracranial study of long-range oscillatory coherence across a frontal-occipital-

hippocampal brain network during visual object processing. Proc Natl Acad Sci. 2008; 105:4399. [PubMed: 18334648]

Smith SM. Fast robust automated brain extraction. Hum Brain Mapp. 2002

Sperling MR. Intracranial Electroencephalography. Elsevier Science Health Science div. 1993

Sperling, MR. Intracranial electroencephalography. In: Ebersole, JS.; Pedley, TA., editors. Current Practice of Clinical Electroencephalography. Lippincott Williams & Wilkins; 2003.

Srinivasan R, Winter WR, Nunez PL. Source analysis of EEG oscillations using high-resolution EEG and MEG. Prog Brain Res. 2006; 159:29–42. http://dx.doi.org/10.1016/S0079-6123(06)59003-X.3d. [PubMed: 17071222]

Thut G, Miniussi C, Gross J. The functional importance of rhythmic activity in the brain. Curr Biol. 2012; 22:R658–R663. [PubMed: 22917517]

Uchida S, Maehara T, Hirai N, Okubo Y, Shimizu H. Cortical oscillations in human medial temporal lobe during wakefulness and all-night sleep. Brain Res. 2001; 891:7–19. [PubMed: 11164805]

Viventi J, Kim DH, Vigeland L, Frechette ES, Blanco JA, Kim YS, Avrin AE, Tiruvadi VR, Hwang SW, Vanleer AC, Wulsin DF, Davis K, Gelber CE, Palmer L, Van der Spiegel J, Wu J, Xiao J, Huang Y, Contreras D, Rogers JA, Litt B. Flexible, foldable, actively multiplexed, high-density electrode array for mapping brain activity in vivo. Nat Neurosci. 2011:1–9.

Voytek B. Shifts in gamma phase–amplitude coupling frequency from theta to alpha over posterior cortex during visual tasks. Front Hum Neurosci. 2010; 4 http://dx.doi.org/10.3389/fnhum.2010.00191.

Walter WG, Dovey VJ. Electro-encephalography in cases of sub-cortical tumour. J Neurol Neurosurg Psychiatry. 1944; 7:57. [PubMed: 21610865]

Wang C. Responses of human anterior cingulate cortex microdomains to error detection, conflict monitoring, stimulus-response mapping, familiarity, and orienting. J Neurosci. 2005; 25:604–613. [PubMed: 15659596]

Wang XJ. Neurophysiological and computational principles of cortical rhythms in cognition. Physiol Rev. 2010; 90:1195–1268. [PubMed: 20664082]

Wilcox, RR. Applying Contemporary Statistical Techniques. Academic Pr; 2003.

Zar, JH. Biostatistical Analysis. 4. Prentice Hall; Upper Saddle River, New Jersey: 1999.

Zaveri HP, Pincus SM, Goncharova II, Novotny EJ, Duckrow RB, Spencer DD, Blumenfeld H, Spencer SS. Background intracranial EEG spectral changes with anti-epileptic drug taper. Clin Neurophysiol. 2010; 121:311–317. [PubMed: 20075002]

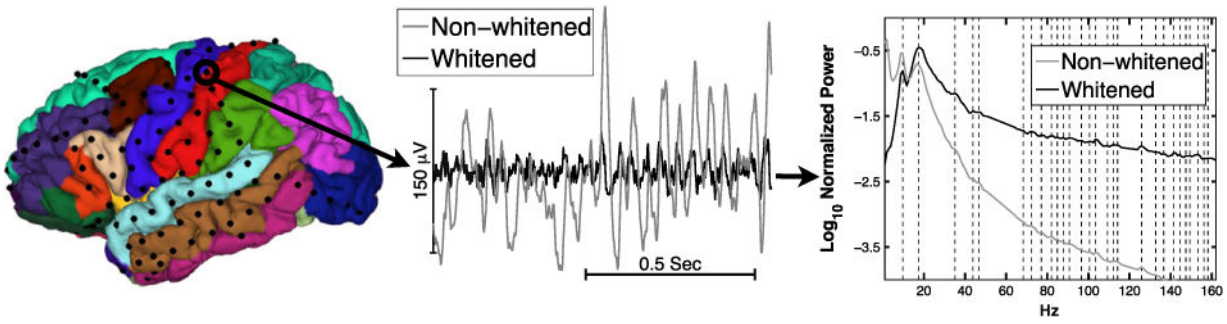

Fig. 1.

[Left] Cortical surface of a single participant, S1, with electrode locations represented as black disks. Different colors indicate different cortical areas according to the Desikan-Killiany atlas. [Middle] One second of resting state activity from a single electrode over S1's left postcentral gyrus, LGd64. The raw time series is shown in gray under the whitened version of the time series. [Right] Trimmed mean spectral power density (SPD) of S1's LGd64 channel before and after whitening. SPD is normalized to unit power across the frequencies of interest before being log transformed. Dashed lines indicate peaks in the whitened SPD. Note that SPD values from 51 to 64 Hz and from 117 to 123 Hz were ignored due to line noise; linear interpolations across those bands are shown.

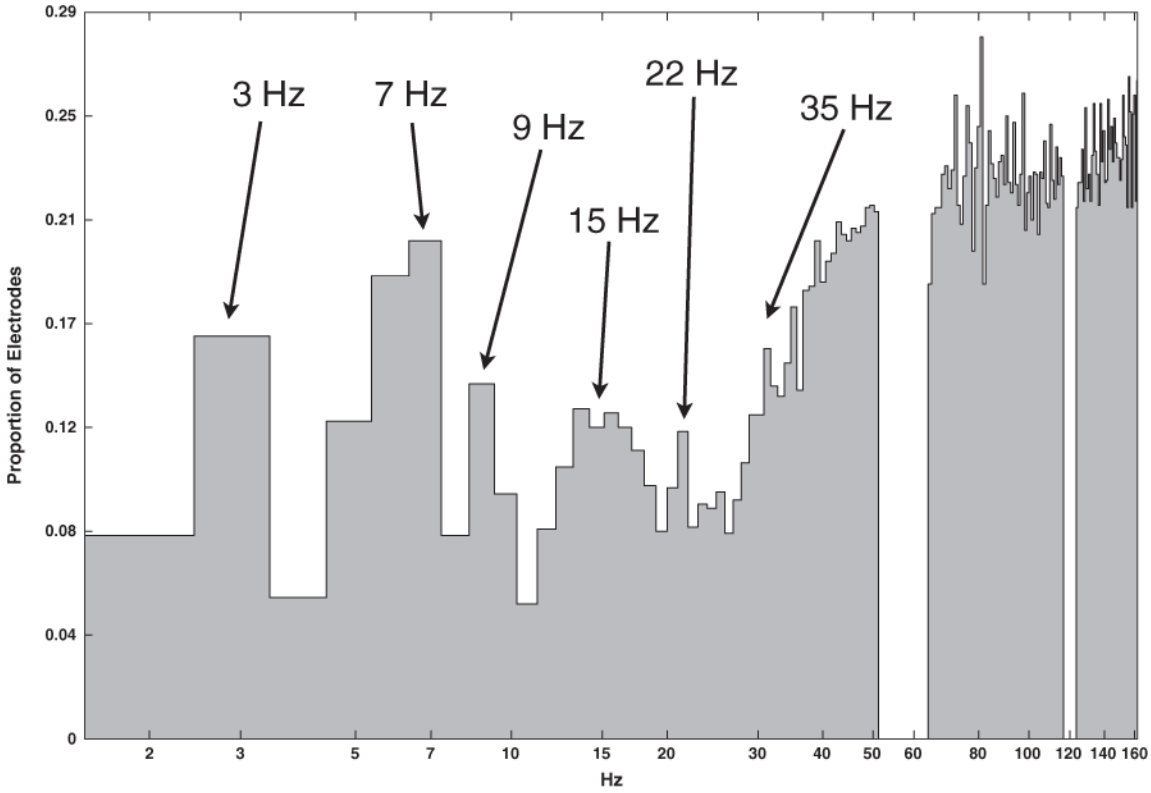

Fig. 2.

Histogram of SPD peaks of whitened data found across all electrodes and participants. Note that Hertz is scaled logarithmically.

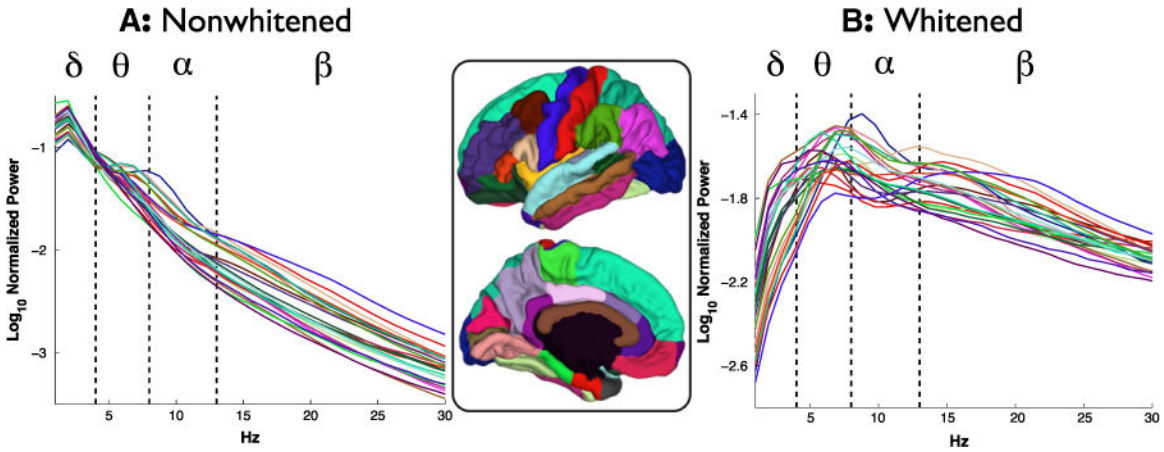

Fig. 3.

Mean SPDs of nonwhitened [A] and whitened [B] data per cortical area across all participants. SPDs are color coded according to cortical area (shown in the middle). Dashed lines indicate conventional delta, theta, alpha, and beta boundaries. Only data from areas with more than three subjects are shown for comparison with Fig. 4.

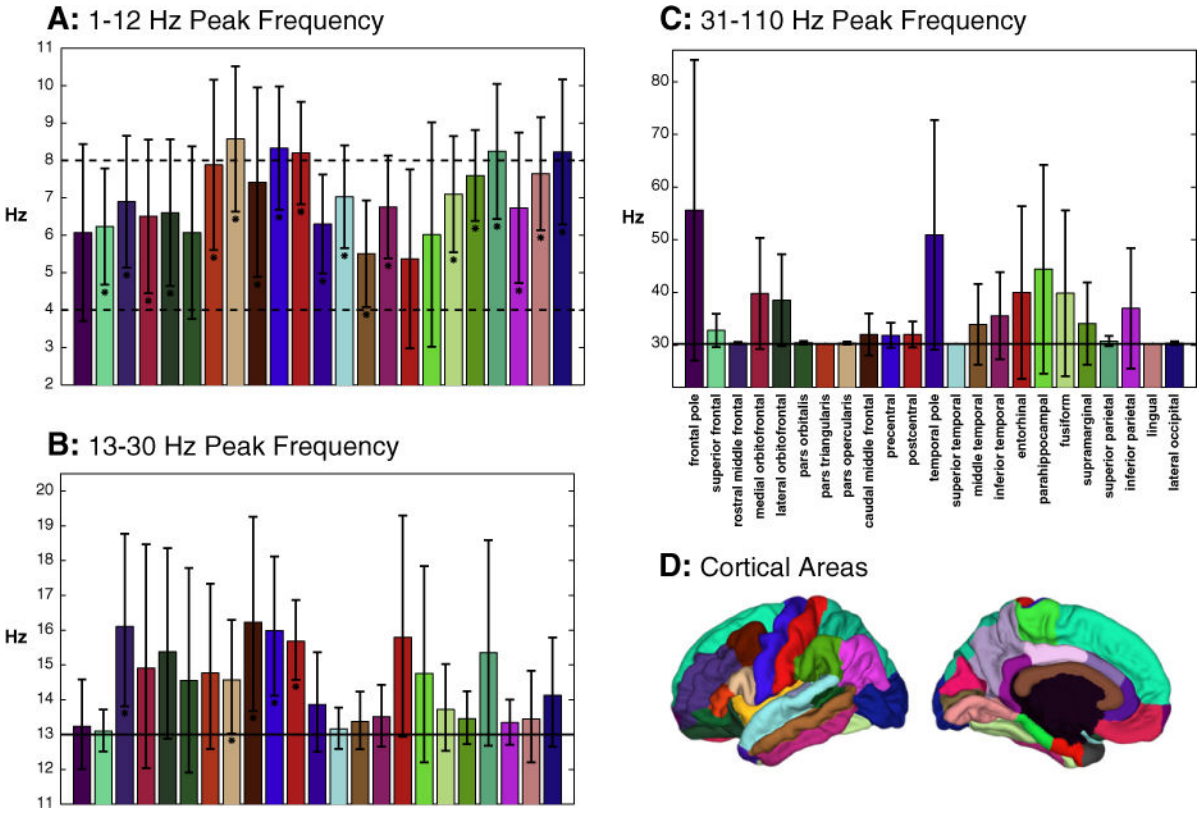

Fig. 4.

Mean frequency that exhibits maximal power in whitened data SPDs across three frequency bands. Errors bars indicate 95% confidence intervals (*t*-distribution assumed, no correction for multiple comparisons). [A] Dashed lines indicate conventional delta, theta, and alpha boundaries. Asterisks below error bars indicate that mean peak frequency is significantly ($p_{adj} < 0.05$ FDR corrected) above delta. No error bars are significantly below alpha after FDR adjustment. [B–C] Solid lines indicate lower boundary of frequency range; no deviation from this line indicates an absence of peaks. Asterisks above error bars indicate significant peaks. Bars are color coded according to cortical area [D] and organized from most anterior to most posterior area.

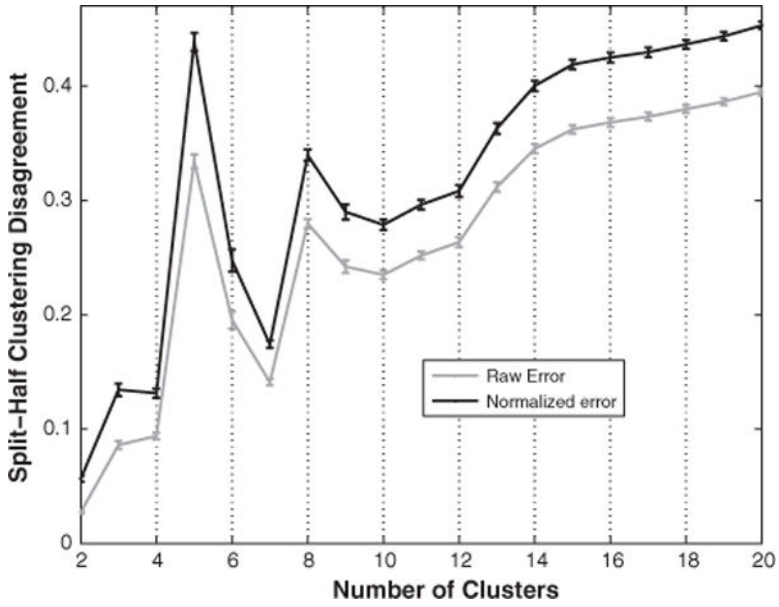

Fig. 5.

Mean clustering disagreement between independent applications of *k*-means to split-halves of all SPDs. A disagreement of 0 means that perfectly compatible clustering solutions were derived. A disagreement of 1 means that completely incompatible solutions were derived. Raw error is normalized by dividing it by the disagreement expected by chance. Error bars are 95% confidence intervals (*t*-distribution assumed).

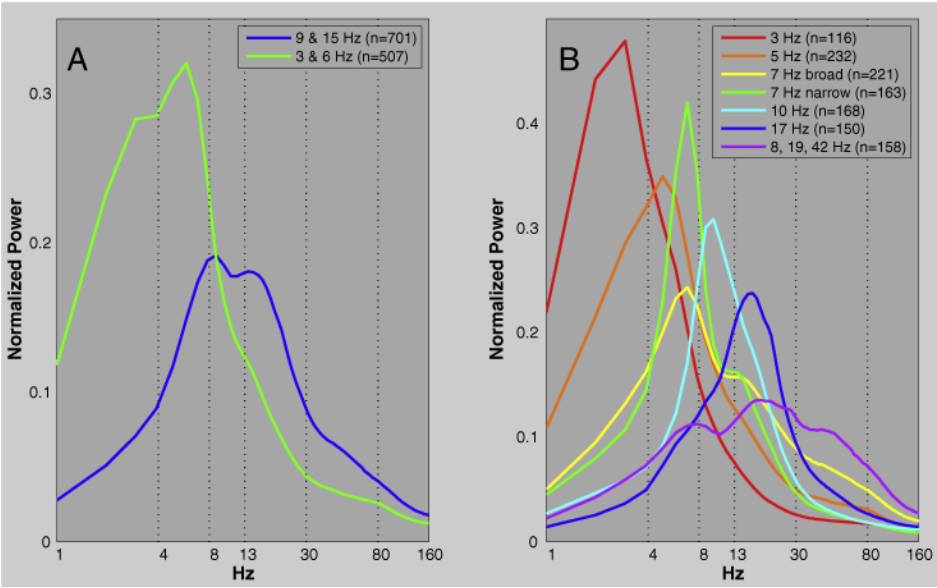

Fig. 6.

SPD centroids of two [A] and seven [B] cluster solutions of all 1208 SPDs. Dashed lines indicate conventional delta, theta, alpha, beta, gamma, and high gamma boundaries. Note that Hertz is logarithmically scaled.

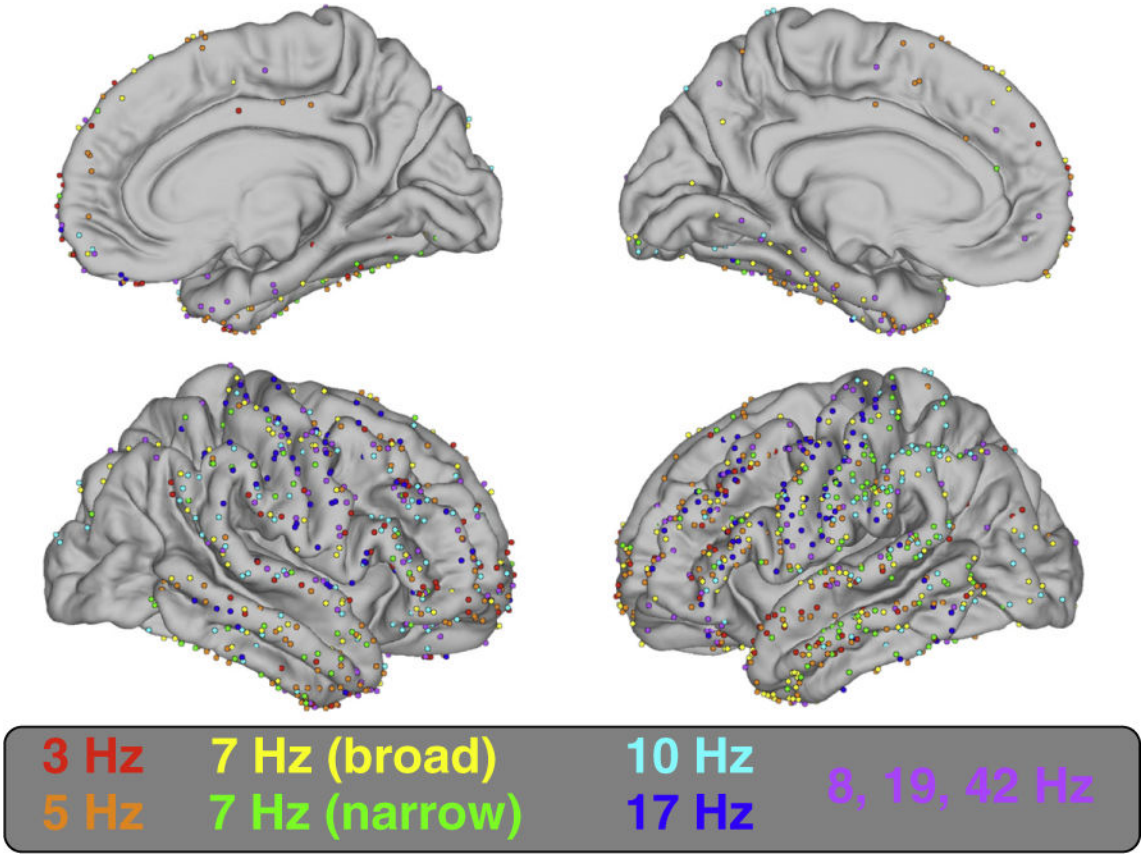

Fig. 7.

Locations of all 1208 electrodes on average cortical surface. Electrodes are color coded to indicate cluster membership (see Fig. 6: B).

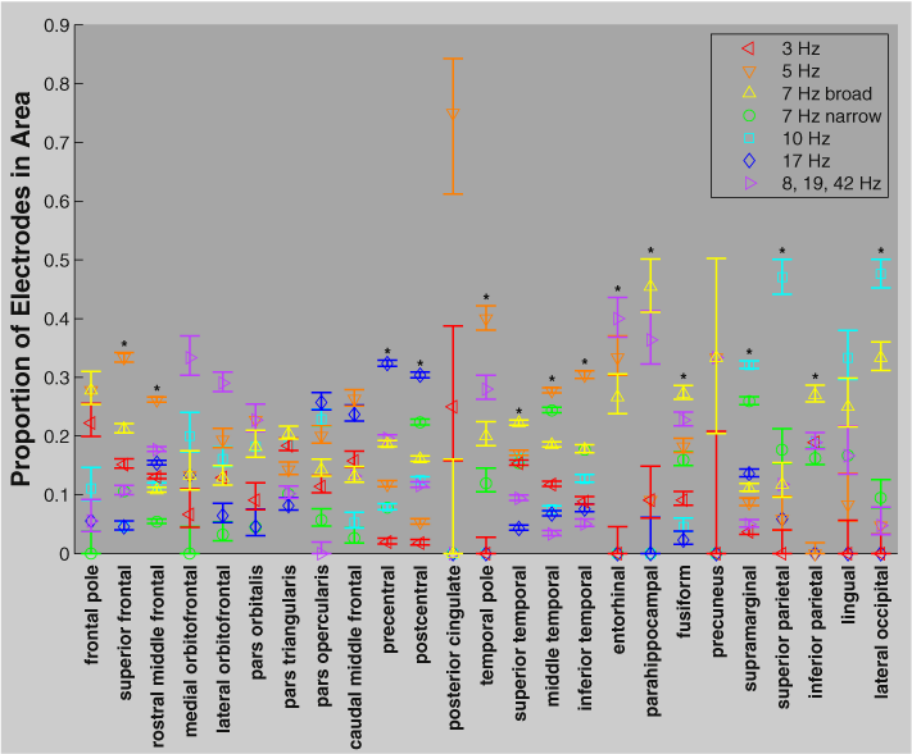

Fig. 8.

Proportions of electrodes belonging to each cluster in various cortical areas (see Fig. 4: D) averaged across participants. Clusters are color coded according to Figs. 6: B & 7. Error bars indicate 68% confidence intervals (Zar, 1999), equivalent to standard error for normally distributed variables. * indicates that some clusters occurred significantly more frequently than others in that area (Chi^2 test, $p_{adj} < 0.05$ FDR corrected for 25 comparisons–Benjamini and Hochberg, 1995). Only areas covered by more than one electrode (out of all 1208) were included in this analysis.